UNIVERSITY OF CALIFORNIA SAN DIEGO

Techno-economic analysis of a Microgrid with solar PV, Battery Energy Storage and Power to Hydrogen (P2H) System

A Thesis submitted in partial satisfaction of the
requirements for the degree
Master of Science

in

Mechanical and Aerospace Engineering

by

Rajat Sethi

Committee in charge:

Professor Jan Kleissl, Chair
Professor Michael Davidson
Professor George Tynan

2020

The Thesis of Rajat Sethi is approved, and it is acceptable in quality and form for publication on microfilm and electronically:

_____

_____

_____

Chair

University of California San Diego

2020

DEDICATION

Dedicated to my family and friends

TABLE OF CONTENTS

Signature Page iii

Dedication iv

Table of Contents v

List of Figures vii

List of Tables viii

Acknowledgements ix

Vita x

Abstract of the Thesis xi

Chapter 1 Introduction 1
1.1 Motivation 1
1.2 Related works 2
1.3 Contribution 5
1.4 Organization 6

Chapter 2 Power to Hydrogen System 7
2.1 Introduction 7
2.2 Electrolyzer Technologies 8
2.3 Hydrogen Storage 10
2.4 Fuel Cells 11

Chapter 3 Modeling 13
3.1 Introduction to HOMER Pro 13
3.2 Mathematical formulation of the Problem 14
3.3 Mathematical Model of Major Components 18
3.3.1 Solar Photovoltaic (PV) Array 18
3.3.2 Battery Bank 19
3.3.3 Diesel Generator 19
3.3.4 Electrolyzer 20
3.3.5 Hydrogen Storage Tank 20
3.3.6 Fuel Cell 20
3.4 Control Strategy 21

Chapter 4 Case Study . . . 23
4.1 Introduction . . . 23
4.2 Structure of the Proposed Microgrid . . . 25
4.3 Scenarios Description . . . 25
4.4 Input Data . . . 29
4.4.1 Solar PV panel . . . 29
4.4.2 Battery Bank . . . 29
4.4.3 Bi-directional Converter . . . 30
4.4.4 Diesel Generator . . . 30
4.4.5 Fuel Cell . . . 31
4.4.6 Electrolyzer . . . 31
4.4.7 Hydrogen Storage Tank . . . 31
4.4.8 Project Economics and other optimization inputs . . . 32

Chapter 5 Results and Discussion . . . 33
5.1 Introduction . . . 33
5.2 Optimization results for each scenario . . . 34
5.3 Comparison of results . . . 39
5.4 Sensitivity analysis . . . 44
5.5 Discussion of results . . . 45

Chapter 6 Conclusions . . . 46

Bibliography . . . 48

LIST OF FIGURES

Figure 4.1: Annual Load Profile for the microgrid in San Diego, CA 23
Figure 4.2: Average Daily Load Profile for the microgrid in San Diego, CA 24
Figure 4.3: Annual Solar Irradiation (GHI) 24
Figure 4.4: Annual Temperature Variation 25
Figure 4.5: Components of proposed microgrid 26
Figure 4.6: Schematic of Scenario 1 27
Figure 4.7: Schematic of Scenario 2 27
Figure 4.8: Schematic of Scenario 3 28
Figure 4.9: Schematic of Scenario 4 28

Figure 5.1: Efficiency versus Output Power for 300 kW and 350 kW Diesel Generators 35
Figure 5.2: Net Present Cost by Component for Scenario 1 36
Figure 5.3: Net Present Cost by Cost Type for Scenario 1 36
Figure 5.4: Net Present Cost by Component for Scenario 2 37
Figure 5.5: Net Present Cost by Cost Type for Scenario 2 37
Figure 5.6: Net Present Cost by Component for Scenario 3 39
Figure 5.7: Net Present Cost by Cost Type for Scenario 3 39
Figure 5.8: Net Present Cost by Component for Scenario 4 40
Figure 5.9: Net Present Cost by Cost Type for Scenario 4 40
Figure 5.10: One week Load Profile (June) 43
Figure 5.11: One week Load Profile (December) 43
Figure 5.12: Cost sensitivity of electrolyzer and fuel cell 44

LIST OF TABLES

Table 4.1: Specifications of PV System 29
Table 4.2: Specifications of Battery Bank 30
Table 4.3: Specifications of Diesel Generator 30
Table 4.4: Specifications of Fuel Cell 31
Table 4.5: Specifications of Electrolyzer 31
Table 4.6: Specifications of Hydrogen Tank 32

Table 5.1: Results for Scenario 1 34
Table 5.2: Results for Scenario 2 37
Table 5.3: Results for Scenario 3 38
Table 5.4: Results for Scenario 4 40
Table 5.5: Simulation results for the proposed scenarios 41

ACKNOWLEDGEMENTS

I would like to thank Professor Jan Kleissl for his unwavering support as my research advisor. Without his guidance and seemingly infinite patience, the research and thesis would not have been possible. You have set an example of excellence as a researcher, mentor, instructor, and role model.

I would like to thank my thesis committee members, Professor Michael Davidson and Professor George Tynan for all of their guidance through this process; your discussion, ideas, and feedback have been absolutely invaluable.

VITA

2014	B.Tech in Mechanical Engineering, Delhi Technological University, Delhi, India
2014-2018	Power Plant Systems Design Engineer, Toshiba Corporation, Japan
2018-2020	Teaching Assistant, University of California San Diego
2019-2020	Energy Algorithm Design Intern, Distributed Solutions Team, EDF Renewables Inc. San Diego
2020	Master of Science, University of California San Diego

PUBLICATIONS

Rajat Sethi, Jan Kleissl, 'Comparison of Short-Term Load Forecasting Techniques', *IEEE Sustech Conference*, 2020.

ABSTRACT OF THE THESIS

Techno-economic analysis of a Microgrid with solar PV, Battery Energy Storage and Power to Hydrogen (P2H) System

by

Rajat Sethi

Master of Science in Mechanical and Aerospace Engineering

University of California San Diego, 2020

Professor Jan Kleissl, Chair

A techno-economic analysis was conducted for a 100% renewable energy-based standalone microgrid system comprising of solar PV, battery energy storage and Power to Hydrogen (P2H) system (comprised of Electrolyzer, Fuel Cell and Hydrogen Storage Tank). Hydrogen is gaining widespread interest globally as an energy carrier as well as a storage medium. This study evaluates the potential of hydrogen systems to utilize (in fuel cells) and store (in the form of compressed hydrogen) excess renewable electricity generated which otherwise would be curtailed. Four scenarios (including a diesel generator only base-case scenario) were investigated for a 25 year project lifetime period to select the most optimal set of energy technologies to meet

load requirements of a microgrid in San Diego, CA. The microgrid had an electrical load of around 2900 kWh/day and peak annual load of 312 kW. The microgrid design optimization tool HOMER Pro® was used to design, model, and simulate the energy technologies and to analyze and compare the energy balance, economics, and environmental emissions amongst the proposed scenarios. A sensitivity analysis was performed to evaluate design robustness against the uncertainty pertaining to fuel cell and electrolyzer costs. The simulation results showed that a hydrogen-battery based renewable hybrid energy storage system minimized total net present cost, and levelized cost of energy technologies. The proposed hybrid energy system has the potential to be deployed to a 100% renewable energy based standalone microgrid system, with low energy generation costs and facilitating in decarbonization efforts.

Chapter 1

Introduction

1.1 Motivation

An increasing number of Renewable Energy (RE) technologies (such as solar, wind, bioenergy, etc.) are being adopted across the world in an effort towards global decarbonization. However, bulk of these RE technologies exhibit variability in electricity generation with an associated uncertainty (dropping of the solar output with the sudden arrival of a cloud or falling of the wind energy generation when wind stops blowing) which is the main challenge in the integration of these RE technologies into the conventional generation systems. Thus, the necessity of large scale energy storage systems which can act as energy reservoirs during periods of excess renewable electricity generation to dispatch during the periods when there is more electricity demand than supply thus providing both upward and downward flexibility. Also, the storage systems will need to be robust enough to do the load shifting on different timescales (miliseconds up to months). Conventional energy storage systems (like pumped hydro storage, battery, flywheels, etc.) have their own merits. However, they all have technical limitations which necessitates the research on innovative approaches to store energy in an environmental friendly way for large capacity systems and for longer discharge durations. Hydrogen has emerged as a

desirable long-term renewable energy storage resource with added benefits of mobility (being transportable) and utilizability. There is numerous ongoing research as well as large scale deployment of hydrogen-based energy technologies underway around the world as described in Section 1.2.

Microgrids (MGs) are expected to form a big part of the decarbonization effort, helping transform the traditional centralized electricity dispatch systems to a more decentralized approach which can be operated both in a non-autonomous (when the system is interconnected to the main grid) and autonomous way (when disconnected from the main grid or is in islanded mode) thereby providing promising ways to enhance grid reliability and resilience. In the cases where it is desirable to isolate the system from the faults in the main grid, or high electricity prices, or for supplying electricity to remote areas, an islanded or a standalone microgrid can be an answer. Such a decentralized system caters to the load requirement of a specific localized area and comprises of local electricity generation sources to meet the localized energy needs. It also comprises of storage systems to ensure system reliability. The main challenge in designing this islanded system is deciding the most optimal set of technologies to be used and sizing them appropriately to make the system reliable and resilient while minimizing the system capital and operational costs.

1.2 Related works

The development of hydrogen production and storage has emerged worldwide as a reliable source for large-scale seasonal storage of electricity. An innovative technology in this regard is the power to hydrogen (P2H) system. Such a system can help in increasing the integration of variable renewable energy (VRE) resources into the energy mix, by avoiding electricity curtailment, electricity grid congestion and by improving system reliability in remote areas or in islanded microgrids.

Previously, many researchers have widely studied RE-based microgrid systems. Dalton et al. [1] analysed the feasibility of RE supply for a stand-alone tourist operation (with over 100 beds) by utilizing the power data from a hotel located in coastal Queensland, Australia. They used HOMER and HYBRIDS software tools and analyzed the net present cost, renewable factor and payback time to compare diesel generator-only, RES-only and RES/diesel hybrid technologies. They highlighted that large-scale systems over 1000 kW were more efficient and economical than multiple small-scale systems ranging between 0.1 and 100 kW. Mamaghani et al. [2] analyzed the application of photovoltaic (PV) panels, wind turbines and diesel generators in a stand-alone hybrid power generation system for rural electrification in Colombia. They modeled and optimized the hybrid system in HOMER to determine the most energy-efficient and cost-effective configuration taking into account net present cost, initial capital cost, and cost of energy as economic indicators. Corsini et al. [3] assessed the energy and environmental performance of H_2 based and desalination water-production systems, in stand-alone power system (SAPS) configuration typical of minor Mediterranean islands, by converting the available RE surplus. These systems were proposed as two effective alternatives for renewable energy seasonal buffering in an island context. Soshinskaya et al. [4] explored the techno-economic potential of renewable electricity-based microgrid serving an industrial-sized drink water plant in the Netherlands. Their results showed a high potential for wind power and solar PV at the site, and the potential for the plant to become 70% and 96% self-sufficient with renewable electricity.

Most of the recent research has focused on maximizing the economic, technological and environmental benefits of microgrid systems [5] because a) the control and operation of the microgrids is decentralized and hence, different from conventional electric power systems which are in most cases, centrally controlled and operated, and b) the generation from the RE resources is fluctuating and heavily influenced by climate and environmental factors. Many research studies have also focused on dealing with energy management systems and controllers for P2H systems, as well design of hybrid P2H-battery systems. Samir et al. [6] reviewed new ways of energy

practice of hybrid energy sources. They presented the physical modelling of the renewable energy resources with numerous methodologies and principles of optimization for hybrid networks. They highlighted that the current trend of optimization for hybrid renewable sources demonstrates that artificial intelligence provides worthy optimization for the microgrid operations without an extensive long-term weather data. Chen et al. [7] proposed a real-time multi-time scale coordinated control scheme to decide the adjustment priority of the distributed generations which has the advantages of good robustness and fast solving speed for stable and economic operation of stand-alone microgrid with hybrid energy storage system comprised of wind power generation units, PV units, and diesel generation units. A research project was carried out by Li et al. [8] on a new concept of primary frequency control with battery in standalone microgrid systems, which also extended the battery service time using dynamic droop method. These research studies highlighted that an optimal energy management system is essential for optimal utilization of different components in a P2H system as well as in optimization of renewable energy storage systems and their role in frequency and voltage control. Shafiullah et al. [9] developed a hybrid model (solar +wind) to investigate the prospects of solar and wind energy for Mid-West region of Western Australia considering production cost, cost of energy, emission production and contribution from renewable energy using HOMER. Their study highlighted that integration of renewables like solar PV and wind with battery storage into existing microgrids comprised of diesel generators can play a significant role to reduce system costs and emissions. Zoulias et al. [10] conducted a techno-economic analysis of the integration of hydrogen energy technologies (electrolyzer, fuel cell, hydrogen storage tank) in RE-based stand-alone power system on the Kythnos Islands, Greece using HOMER tool. They analyzed the size, cost and operational characteristics of the PV-hydrogen system in comparison to the already existing PV-diesel one. Their study highlighted that replacement of fossil fuel based gensets with hydrogen technologies is technically feasible. Dawood et al. [11] conducted the techno-economic feasibility of RE-based systems using hydrogen as energy storage for a stand-alone/off-grid microgrid for a remote

community in Australia by considering the energy balance and techno-economic optimization. They used HOMER for their analysis and showed that the hydrogen-battery hybrid energy storage system can be a cost-effective option for a stand-alone microgrid and that this system has significant potential in electrifying remote communities with low energy generation costs and emissions. Colbertaldo et al. [12] analyzed the California power system for the feasibility of hydrogen as the primary storage means for balancing energy supply and demand and to estimate the sizes for electrolyzer and fuel cell systems in 100% RE scenarios driven by large additions of wind and solar capacities. Their study showed that the transition to full RE system requires a massive increase in both solar and wind generation, as well as hydrogen storage installations. Furthermore, the integration of hydrogen-based storage systems with existing battery storage helps to independently scale power and energy capacities of the system for massive and long duration energy storage.

1.3 Contribution

The primary objective of this study was to assess the relative merits and demerits of various options for energy storage for a standalone microgrid in San Diego, California with intermittent renewable electricity generating systems comprised of solar photovoltaic (PV) and including hydrogen battery based hybrid storage systems. The insights from this study will be useful in gaining a sense of the prospects of various types of renewable energy ”buffer storage” systems in the California context.

The specific goals of this study were as follows:

- To model and simulate a set of 100% RE scenarios (battery based, hydrogen based and hybrid combination of battery and hydrogen based) for a stand-alone microgrid in San Diego, California and compare with base-case scenario (electricity supply from diesel generators)

- To evaluate the economical and technical feasibility of using battery and hydrogen hybrid storage combination for this microgrid system for a period of 25 years
- To determine extent of excess curtailment of renewable electricity (from solar PV) that can be avoided by integration of a power to hydrogen technology in this microgrid system
- To determine the extent of system autonomy by using a hydrogen and battery hybrid energy storage system for this microgrid

1.4 Organization

The methodology followed in this study is organized as follows: Chapter 2 is dedicated to describing the different technological components in a power to hydrogen (P2H) system considered for the present study. In Chapter 3, the simulation tool HOMER Pro, used for modeling and optimization of the various energy technologies is described, as well as the physical model of these energy technologies is explained. Chapter 4 is devoted to describing the various scenarios proposed and analyzed in this study as well as the scenario inputs for conducting scenario-specific simulations using HOMER Pro. In Chapter 5, the optimization results for each of the proposed scenarios as well as sensitivity analysis results are discussed. Finally, in Chapter 6, conclusions of this study are drawn and future work in proposed.

Chapter 2

Power to Hydrogen System

2.1 Introduction

The power to hydrogen (P2H) system is based on absorption of excess renewable electricity by electrolyzers to generate hydrogen which can have several uses. It can be consumed by the fuel cells, stored in hydrogen tanks, injected in gas grids or combined with carbon di-oxide to generate synthetic methane. Rather than curtailing the excess generation, a P2H system acts as a carrier to convert this electricity surplus to generate a chemical energy carrier (like hydrogen).

In this study, the generated hydrogen gas is considered to be stored in an energy storage medium like hydrogen storage tanks which are similar to batteries but use compressed hydrogen as the energy carrier. The stored hydrogen in the tanks can be utilized by a fuel cell to generate electricity. Thus, a P2H system comprises of three main components, the electrolyzer (to generate hydrogen from excess electricity), hydrogen tank (to store hydrogen to use in the system when required) and fuel cell (to convert stored hydrogen into electricity). This chapter discusses the different technologies used in the P2H process.

2.2 Electrolyzer Technologies

The conversion of electricity into chemical energy is the core element of P2H systems and is performed by the process of water electrolysis. The process involves applying an electric potential to the two electrodes which causes the water to split into hydrogen and oxygen components, which are formed at the cathode and anode respectively. The electrolysis process is represented by the reaction equation:

$$H_2O \rightarrow 2H_2 + O_2 \qquad \Delta H^{o} = 286\,kJ/mole\,(at\,25^{\circ}C,\,1\,bar)$$

In addition to the two electrodes, the electrolyzer is also composed of an electrolyte which is capable of ion conduction, and a diaphragm which behaves as an electric isolator and keeps the evolving gases in the above reaction separate in order to avoid a flammable mixture. The electrolyzers used in the P2H systems have special requirements:

- Highly dynamic to follow the fluctuating power input from renewable sources
- High efficiency to avoid unnecessary energy losses
- To allow for stand-by mode with low energy consumption
- Long lifetime and low investment cost to allow for economical hydrogen production

Depending upon the electrolyte used, the electrolyzers can be categorized as

- Alkaline water electrolyzers with a liquid alkaline electrolyte
- Proton exchange membrane (PEM) electrolyzers with a proton-conducting polymer electrolyte membrane
- High temperature electrolysis with a solid oxide electrolyte

Alkaline electrolyzers have an aqueous alkaline electrolyte of potassium hydroxide (KOH) with 20-40% wt. KOH concentration and conducts OH^- ions, operate between 70°C and 140°C

with pressures varying between 1 and 200 bar [13]. Typically they achieve stack efficiencies of between 60-71% (HHV). The commercially available modules have capacities of upto 760 Nm^3/h. Main issues involved with using these electrolyzers in P2H systems is their minimal part-load capability. The minimal load is limited by the gas conductivity of the electrolyzer diaphragm, where the gas conductivity causes critical H_2 concentration in the O_2 stream for low gas flows. Also, in terms of dynamics, alkaline electrolyzers are slower than PEM electrolyzers due to inertia of the periphery [14]. The cost of these electrolyzer systems is estimated in the range of $1000/kW which includes power supply, system control and gas drying and is expected to drop by 40-50% in the near future [15].

PEM electrolyzers have been developed over the last 20 years. The technology is based on utilization of a proton-conducting polymeric membrane as the electrolyte and diaphragm combined in one element. Operating temperatures are limited to about 80°C due to the polymeric material [16]. The membrane allows for low part loads due to its impermeability of gases. Hydrogen can be produced at pressures of up to 150-200 bar [17]. The cell efficiency of these electrolyzers is of the same magnitude as the alkaline electrolyzers, however their stack efficiency is lower. These electrolyzers have the advantage of simple design and typically reach high efficiencies between 65 - 85% (HHV) and are ideal for fast load changes. Major issue with these electrolyzers is the related costs. The noble catalysts (Pt, Ir, Ru) and the need for titanium-based bipolar plates leads to a current investment costs of about $2500/kW. There is potential for cost-reduction in future years by using alternative materials, improving stack efficiencies and exploiting the effect of technology being scaled up industrially.

In high-temperature solid oxide electrolyzers, the electrolyte is a cermaic electrolyte, or a solid oxide (solid oxide electrolysis cell, SOEC) which consists of O^{2-} conducting yttria-stabilized zirconium oxide [13]. SOEC is operated at temperatures in the range of 700-1000°C with steam instead of liquid water. The electric efficiency of such cells can exceed even 100% since only a part of the enthalpy required for water-splitting is provided by electricity and the rest can

be provided by a high-temperature heat source. For such electrolyzers, constant operation is preferable since ceramics can undergo thermal stress which limits their use for P2H applications since the flexible mode of operation requires numerous start-up and shut-down cycles.

2.3 Hydrogen Storage

The hydrogen produced by the electrolyzer can be stored in the gaseous form at high pressures in the hydrogen storage tank. The gaseous form has the advantage of simplicity in transportation of gaseous fuel, excellent dormancy characteristics, and low infrastructure impact along with added benefits of large-scale, low-cost storage. Storing a kg of hydrogen at 100 kPa and 25 °C requires a tank of volume around 12 m^3. Compressing hydrogen to pressures of upto 350 bar decreases the required storage volume by 99.6% [18]. Further pressure increase lowers the storage volume but leads to increasing compression work and safety concerns. In order to save compression energy, a buffer tank can be installed after the electrolyzer and compression can start when the tank is at full charge [18]. Compressed hydrogen can be stored in closed tanks with volumetric densities of around 20-50 kg/m^3. The size of long-term hydrogen storage tank is decided based on the availability and seasonal variation of renewable power sources and the desired system autonomy.

Hydrogen can also be stored in liquid form at extremely low temperatures, however to be liquified, it can take upto 40% of energy content of hydrogen [18]. Liquid hydrogen is in demand in applications with high level of desired purity like chip industry or when high storage density is desired like in aerospace applications.

2.4 Fuel Cells

Depending on the choice of fuel and the electrolyte, the fuel cell (FC) technologies can be categorised as:

- alkaline (AFC)
- phosphoric acid (PAFC)
- solid oxide (SOFC)
- molten carbonate (MCFC)
- proton exchange membrane (PEMFC)
- direct methanol (DMFC)

In this study, PEMFC type fuel cell is considered. These fuel cells utilize polymer electrolyte membranes to conduct protons for ion exchange purposes. During operation, PEMFC consumes hydrogen in the anode chamber where it is oxidized while the oxygen in the cathode chamber is reduced. The cell reaction is:

$$Cathode : O_2 + 4H^+ + 4e^- \rightarrow 2H_2O$$

$$Anode : 2H_2 \rightarrow 4H^+ + 4e^-$$

$$Overall : 2H_2 + O_2 \rightarrow 2H_2O$$

The products of the reaction in the fuel cell are water, electricity and heat. The catalyst in these cells is usually comprised of platinum nanoparticles very thinly coated onto carbon paper. The catalyst is rough and porous so that the maximum surface area of the platinum can be exposed to hydrogen and oxygen. These fuel cells operate at low temperatures between 60-100°C, and can achieve electrical efficiencies between 40-65% [19]. Development of low-cost catalysts greatly

helped in reducing the overall costs of this fuel cell (for example, the amount of platinum used in PEMFC reduced around 10-100 fold [20]) and the costs are expected to reduce even further in the near future [21].

Chapter 3

Modeling

3.1 Introduction to HOMER Pro

The Hybrid Optimization of Multiple Energy Resources (HOMER) Pro is a simulation tool used widely in the design of microgrid systems and to help in comparison of different power technology components across a wide range of applications. HOMER Pro models a component's physical behaviour and its life-cycle cost, which is the total cost of installing and operating the component over its lifetime. HOMER Pro allows a designer to compare different technology combinations based on their technical and economic merits. Also, it allows for conducting sensitivity analysis for different input variables which helps to quantify the effect of change of these variables. HOMER Pro can model both grid-connected and off-grid power systems serving electrical and thermal loads with any combination of technologies like solar photovoltaic (PV) modules, battery energy storage, diesel generators, fuel cells, electrolyzers, hydrogen storage, etc. HOMER Pro thus performs three principal tasks which are simulation, optimization and sensitivity analysis. In the simulation process, it performs the calculations for a system configuration for each hour of the year to determine the technical feasibility and life-cycle cost. In the optimization process, it evaluates different combinations of the specified technologies based on the system

constraints and searches for the most optimal combination of technologies that minimizes the total Net Present Cost. In the sensitivity analysis process, it evaluates multiple case studies to gauge the effect of changes in the input parameters (mostly these are the parameters over which a designer has no control - like the fuel price). These can be then plotted in the form of surface plots, line plots, spider plots to visualize the changes graphically. For finding optimal size of solar photovoltaic (PV), Battery Storage, and Converters, HOMER Optimizer requires the information about site location, electrical load to be served and some estimates of costs for these components. The optimizer then uses a derivative free optimization algorithm to find the least cost combination of components for meeting the electric load and user defined constraints while searching from an essentially infinite space of component sizes till the user defined convergence criteria is met (these could be: maximum simulations per optimization, system design precision which is the maximum relative precision of decision variables allowed for convergence, maximum relative error in net present cost (NPC) required for convergence, and focus factor value to control the rate of convergence). For sizing generators and electric heaters however, it uses a modified grid search algorithm which requires the user to enter specific component sizes (user-defined search space) and then iterates over the search space to provide the best candidate solution based on the search space and the dispatch algorithm selected.

3.2 Mathematical formulation of the Problem

The objective function of HOMER Pro is the minimization of the total Net Present Cost (NPC) or also known as life-cycle cost. NPC is the present value of all the costs the system incurs (including costs for installation and operation of all components) over its lifetime, minus the present value of all the revenue it earns over its lifetime. Costs include capital costs, replacement costs, operation and maintenance (O&M) costs, fuel costs, and the costs of buying power from the grid (which is not applicable in the current study though). Revenues include salvage value

and grid sales revenue (which, in this case, is zero as there is no connection to the utility grid). During the simulation, HOMER Pro calculates each of these costs along with the salvage value and any other costs or revenues, to arrive at each component's annualized cost given by equation 3.1 . Annualized cost is the hypothetical annual cost that if it occurred each year of the project lifetime would yield a net present cost equivalent to that of all the individual costs and revenues associated with that component over the project lifetime.

$$C_{\text{ann,i}} = \sum_i C_{\text{capital,i}} + C_{\text{O\&M,i}} + C_{\text{replacement,i}} + C_{\text{fuel,i}}, \tag{3.1}$$

where $C_{\text{ann,i}}$ is the annualized cost, $C_{\text{capital,i}}$ is the capital cost, $C_{\text{O\&M,i}}$ is the fixed O&M cost, $C_{\text{replacement,i}}$ is the replacement cost , and $C_{\text{fuel,i}}$ is the fuel cost of the component i.

HOMER Pro sums these annualized costs of each component, along with any miscellaneous costs, such as penalties for pollutant emissions in order to arrive at the value of total annualized cost of the system denoted by $C_{\text{ann,tot}}$.

This value is an important one because HOMER Pro then uses it to calculate the two principal economic figures of merit for the system: the total net present cost and the levelized cost of energy. HOMER Pro uses equation 3.2 to calculate the total net present cost C_{NPC}.

$$C_{\text{NPC}} = \frac{C_{\text{ann,tot}}}{CRF(x, R_{\text{proj}})}, \tag{3.2}$$

where $C_{\text{ann,tot}}$ is the total annualized cost, x is the annual real discount rate, R_{proj} is the project lifetime, and CRF is the capital recovery factor given by the equation 3.3

$$CRF(x, R) = \frac{x(1+x)^R}{(1+x)^R - 1}, \tag{3.3}$$

where R is the project lifetime (in years).

The NPC condenses all these costs and revenues occuring over a system's lifetime into

one lump sum in today's value, with future cash flows discounted into the present using the discount rate which is a parameter that can be specified by the designer. HOMER Pro assumes that all prices escalate at the same rate over the project lifetime. Inflation can then be factored out of the analysis by using a real discount rate (inflation adjusted) instead of a nominal discount rate. [22]. Both the nominal discount rate and inflation rate can be specified by the designer. It then uses equation 3.4 to determine the real discount rate.

$$x = \frac{x' - f}{1 + f}, \tag{3.4}$$

where x is the real discount rate, x' is the nominal discount rate and f is the inflation rate.

For calculating the levelized cost of energy, HOMER Pro uses equation 3.5.

$$COE = \frac{C_{\text{ann,tot}}}{E_{\text{prim}} + E_{\text{def}} + E_{\text{grid,sales}}}, \tag{3.5}$$

where E_{prim} is the primary load, E_{def} is the deferrable load that the system serves per year and $E_{\text{grid,sales}}$ is the amount of electrical energy sold to the grid each year. The levelized cost of energy is then the average cost per kilowatt hour of electrical energy produced by the system.

HOMER Pro runs the optimization in a way that minimizes the net present cost of the system. The minimisation procedure is constrained by inequalities 3.6–3.9:

$$P_{\text{shortage}} \leq 0.01\, P_{\text{load}}, \tag{3.6}$$

$$f_{\text{PV}} \geq 0.50\, E_{\text{gen}}, \tag{3.7}$$

$$\gamma_{\text{load,t}} \geq 0.1\, P_{\text{load,t}} \tag{3.8}$$

$$\gamma_{\text{peak load}} \geq 0.01\, P_{\text{load}} \tag{3.9}$$

where P_{shortage} is the total capacity shortage, P_{load} is the total electrical load demand, f_{PV} is the

PV fraction (in %), E_{gen} is the electricity generation, $\gamma_{\text{load,t}}$ is the operating reserve as a percent of load in the current time step t, $P_{\text{load,t}}$ is the electrical load in the current time step t, $\gamma_{\text{peak load}}$ is the operating reserve as a percent of annual peak load, P_{load} is the total annual electrical load. It is to be noted that the parameter values of 0.01, 0.50, 0.1 and 0.01 in equations (3.6 - 3.9) respectively have been chosen for this study by the author. However, they could be altered for a different design setting.

The PV fraction shown in equation 3.6 can be calculated by using the equation 3.10:

$$f_{\text{PV}} = 1 - \frac{E_{\text{non ren}} + H_{\text{non ren}}}{E_{\text{served}} + H_{\text{served}}} \tag{3.10}$$

where $E_{\text{non ren}}$ is the annual non-renewable electricity production, $H_{\text{non ren}}$ is annual non-renewable thermal production, E_{served} is the annual electric load served, H_{served} is the annual thermal load served. No thermal loads are considered for this study.

HOMER Pro also calculates the operating reserve for each time step to ensure that enough dispatchable capacity is available to keep the operating reserve equal to or greater than the required operating reserve. The required operating reserve is the minimum amount of operating reserve that the system must be capable of providing. This is used to ensure the system reliability during sudden increase or decrease of loads or PV generation. HOMER Pro records any shortfall as a capacity shortage. The operating reserve denoted by $\gamma_{\text{load,t}}$, $\gamma_{\text{peak load}}$ is used in equations 3.11, 3.12 to calculate the required operating reserve in the AC and DC bus at each time step.

$$L_{\text{res, AC}} = \gamma_{\text{load,t}} L_{\text{prim, AC}} + \gamma_{\text{peak load}} \hat{L}_{\text{prim, AC}} \tag{3.11}$$

$$L_{\text{res, DC}} = \gamma_{\text{load,t}} L_{\text{prim, DC}} + \gamma_{\text{peak load}} \hat{L}_{\text{prim, DC}} \tag{3.12}$$

where $L_{\text{res, AC}}$ is the required operating reserve on the AC bus, $L_{\text{prim, AC}}$ is the average AC primary load in the current time step, $\hat{L}_{\text{prim, AC}}$ is the highest AC primary load experienced by the system

during the year, $L_{\text{res, DC}}$ is the required operating reserve on the DC bus , $L_{\text{prim, DC}}$ is the average DC primary load in the current time step, and $\hat{L}_{\text{prim, DC}}$ is the highest DC primary load experienced by the system during the year.

The total NPC is HOMER Pro's main economic output, and the best candidate solution would be the one that results in the lowest total NPC at the start of the project, while satisfying all the input constraints.

3.3 Mathematical Model of Major Components

For sizing optimization using HOMER Pro, modelling of energy system components is essential to evaluate the performance under different scenarios. Mathematical modelling of the proposed energy system components is explained below.

3.3.1 Solar Photovoltaic (PV) Array

The power output of the PV array (P_{PV}) is calculated using

$$P_{\text{PV}} = Y_{\text{PV}} * x_{\text{PV}} * \frac{G_{\text{T}}}{G_{\text{T,STC}}} * [1 + \alpha_{\text{P}} * (T_{\text{c}} - T_{\text{c,STC}})], \tag{3.13}$$

where Y_{PV} is the the rated capacity of the PV array (kW), x_{PV} is the PV derating factor (%), G_{T} is the solar radiation incident on the PV array in the current time step (kW/m^2), $G_{\text{T,STC}}$ is the the incident radiation at standard test conditions (1 kW/m^2), α_{P} is the temperature coefficient of power (%/°C), T_{c} is the PV cell temperature in the current time step (°C), $T_{\text{c,STC}}$ is the the PV cell temperature under standard test conditions (25 °C).

The rated capacity accounts for both the area and the efficiency of the PV module, so neither of those parameters appear explicitly in HOMER Pro . The derating factor is a scaling factor meant to account for effects of dust on the panel, wire losses, or anything else that would cause the output of the PV array to deviate from that expected under rate conditions. The maximum

power point (the voltage at which the array power output is maximized) depends on the solar radiation and the temperature. A maximum power point tracker (MPPT) is a solid-state device placed between the PV array and the rest of the DC components of the system that decouples the array voltage from that of the rest of the system, and ensures that the array voltage is always equal to the maximum power point. By ignoring the effect of the voltage to which the PV array is exposed, HOMER Pro effectively assumes that a MPPT is present in the system [22]. The PV cell temperature is the temperature of the PV cells. HOMER Pro calculates the cell temperature in each time step and use it in calculating the power output of the PV array [23].

3.3.2 Battery Bank

The battery bank is a collection of one or more individual batteries. HOMER Pro models a single battery as a device capable of storing a certain amount of DC electricity at a fixed round-trip energy efficiency (RTE), with limits as to how quickly it can be charged or discharged, how deeply it can be discharged without causing damage, and how much energy can cycle through it before it needs replacement.

3.3.3 Diesel Generator

The generator consumes fuel to produce electricity and also, produces heat which can be used in Combined Heat and Power (CHP) applications. The principal physical properties of the generator are its maximum and minimum electrical power output, its expected lifetime in operating hours, the type of fuel it consumes, and its fuel curve, which relates the quantity of fuel consumed to the electrical power produced. HOMER Pro assumes the fuel curve is a straight line with a y-intercept and uses equation 3.14 for the generator's fuel consumption rate F.

$$F = F_0 * Y_{\text{gen}} + F_1 * P_{\text{gen}} \tag{3.14}$$

where F_0 is the fuel curve intercept coefficient , Y_{gen} is the rated capacity of the generator (kW), F_1 is the fuel curve slope, P_{gen} is the electrical output of the generator (kW).

3.3.4 Electrolyzer

An electrolyzer consumes electricity to generate hydrogen via the electrolysis of water. In HOMER Pro, the user specifies the size of the electrolyzer, which is a decision variable, in terms of its maximum electrical input. The user also indicates whether the electrolyzer consumes AC or DC power, and the efficiency with which it converts that power to hydrogen. HOMER Pro defines the electrolyzer efficiency as the energy content (based on higher heating value) of the hydrogen produced divided by the amount of electricity consumed.

3.3.5 Hydrogen Storage Tank

In HOMER Pro, the hydrogen tank stores hydrogen produced by the electrolyzer for later use in a hydrogen-fueled generator, or fuel cell. The user specifies the size of the hydrogen tank, which is a decision variable in terms of the mass of hydrogen it can contain. HOMER Pro assumes that the process of adding hydrogen to the tank requires no electricity, and that the tank experiences no leakage. The user can specify the initial amount of hydrogen in the tank either as a percentage of the tank size or as an absolute amount in kilograms. It is also possible to require that the year-end tank level must equal or exceed the initial tank level.

3.3.6 Fuel Cell

Fuel Cell systems are very clean, generate no emissions and are characterized by high efficiency. Hydrogen is the primary fuel of fuel cell systems that convert the stored energy of hydrogen fuel directly into electricity with the help of an oxidant used in fuel cells such as oxygen from the air. For this study, proton exchange membrane (PEMFC) is chosen since it has a reliable

performance under unbalanced hydrogen supply. In HOMER Pro, the user specifies the size of the fuel cell, which is a decision variable, in terms of its maximum electrical output.

3.4 Control Strategy

A dispatch control strategy is a set or rules that govern the operation of the system components. HOMER Pro can model two dispatch strategies - cycle charging and load following. Which strategy is optimal depends on many factors, including the sizes of the generators and battery bank, the price of fuel, the O&M cost of the generators, the amount of renewable power in the system, and the character of the renewable resources. The user has the option to model both, and HOMER Pro will then simulate each system using both dispatch strategies and the user will be able to see which is optimal.

Under the load following strategy, whenever a generator is needed it produces only enough power to meet the primary load. Lower-priority objectives such as charging the storage bank or serving the deferrable load are left to the renewable power sources. Load following tends to be optimal in systems with a lot of renewable power, when the renewable power output sometimes exceeds the load.

Under the cycle charging strategy, whenever a generator has to operate to serve the primary load, it operates at full capacity with surplus electrical production going towards the lower-priority objectives such as, in order of decreasing priority: serving the deferrable load, charging the storage bank, and serving the electrolyzer. Cycle charging tends to be optimal in systems with little or no renewable power.

For deciding load priority, HOMER Pro makes a separate set of decisions regarding how to allocate the electricity produced by the system. The presence of both an AC and a DC bus complicates these decisions somewhat. HOMER Pro assumes that electricity produced on one bus will go first to serve primary load on the same bus, then primary load on the opposite bus,

then deferrable load on the same bus, then deferrable load on the opposite bus, then to charge the battery bank, then to grid sales, then to serve the electrolyzer, and then to the dump load, which could optionally serve the thermal load.

Chapter 4

Case Study

4.1 Introduction

Load dataset (15 minute resolution) for an office building in San Diego, CA with daily AC load of 2900 kWh and peak load of 312 kW provided by EDF Renewables has been used. The load profile is shown in Figure 4.1. The overall demand is higher in the summer months of July-Sept with the peak load occurring in August and the least average load occurs in January.

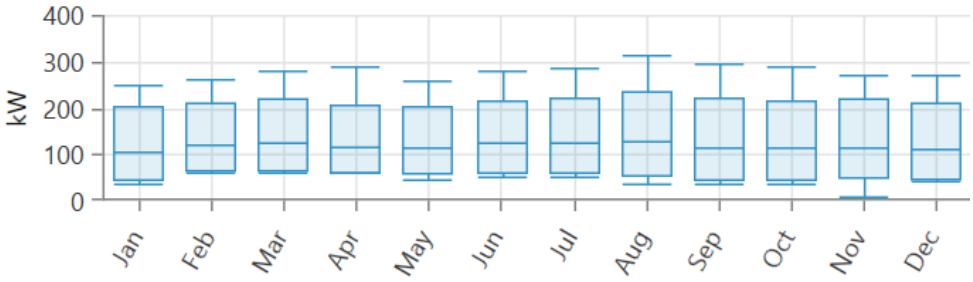

Figure 4.1: Annual Load Profile for the microgrid in San Diego, CA

The average daily load profile is shown in Figure 4.2. The load profile is typical of an office building with peak loads observed between the core working hours from 9AM to 3PM and relatively low loads observed in early morning and late evening hours.

For solar irradiation, the modeling tool uses the solar resources data as downloaded from

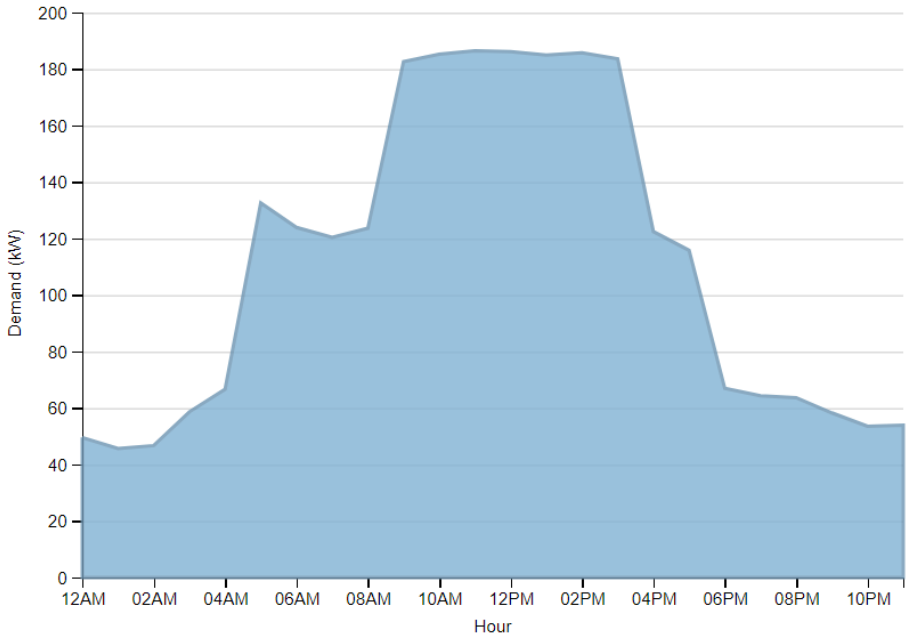

Figure 4.2: Average Daily Load Profile for the microgrid in San Diego, CA

NASA Surface Meteorology and Solar Energy database. By entering the latitude and longitude (32°59.5' N ,117°4.6' W) for the office building site in San Diego, CA, the solar resource shown in Figure 4.3 has been generated. The scaled average annual global horizontal solar irradiation is 5.07 kWh/m^2/day. The clearness index which is a measure of the fraction of solar radiation that is transmitted through the atmosphere to strike the earth is also plotted in the same figure. It has a high value under clear, sunny conditions, and a low value under cloudy conditions.

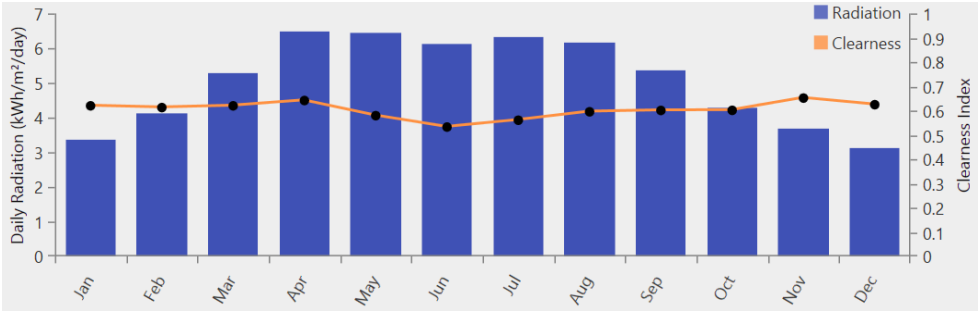

Figure 4.3: Annual Solar Irradiation (GHI) in San Diego, CA

The temperature data for the site was also imported from NASA Surface Meteorology and

Solar Energy database and is shown in Figure 4.4. The average annual temperature is 17.65°C.

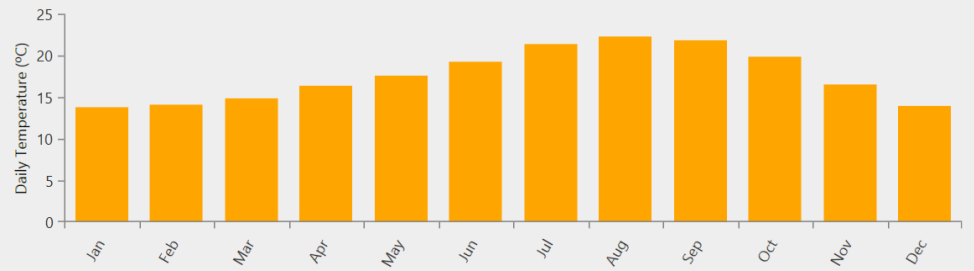

Figure 4.4: Annual Temperature variation in San Diego, CA

4.2 Structure of the Proposed Microgrid

The autonomous microgrid system under consideration consists of solar photovoltaic (PV) panels, a battery energy storage system (BESS) made of Lithium-ion battery, a diesel generator (with a backup generator), and a power to hydrogen system (P2H) comprised of electrolyzer, H_2 storage tank and fuel cell. The system is illustrated in Figure 4.5

4.3 Scenarios Description

For this study, four scenarios are envisaged for the standalone microgrid operation. These were investigated for a 25 year project lifetime period using HOMER Pro to select the most optimal set of energy technologies to meet load requirements of the microgrid by comparing the energy balance, economics and emissions amongst these scenarios.

- Scenario 1 (Base-case): 2 diesel Generators
- Scenario 2: Solar PV and Lithium-ion Battery Storage
- Scenario 3: Solar PV and P2H system (Hydrogen from Fuel Cell, Hydrogen Storage Tank, Electrolyzer)

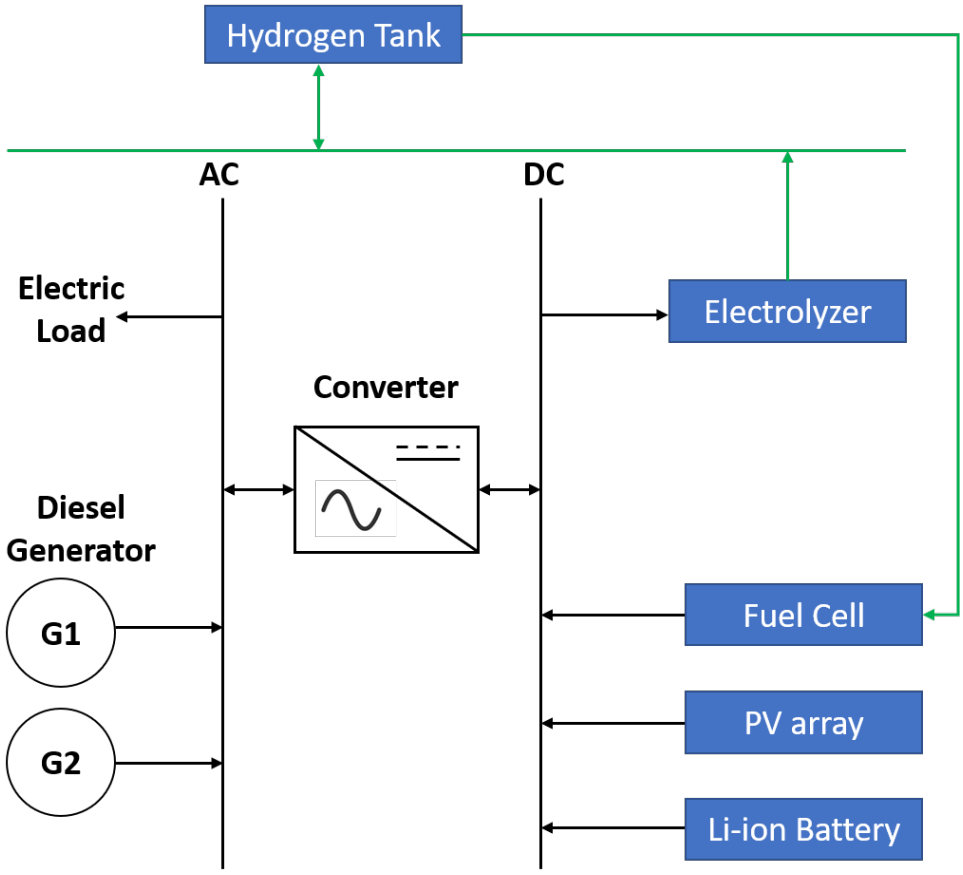

Figure 4.5: Components of proposed microgrid

- Scenario 4: Solar PV, Li-ion Battery Storage and P2H system (Hydrogen from Fuel Cell, Hydrogen Storage Tank, Electrolyzer)

The schematic of Scenario 1 is shown in Figure 4.6. It consists of the two diesel generators of 300 kW capacity each. One is the primary generator and the other is a standby generator for meeting peak loads or to be used as a backup. Both generators are connected to the AC bus.

The schematic of Scenario 2 is shown in Figure 4.7. It is a 100% renewable power system and consists of solar PV and Li-ion battery bank with load following (LF) dispatch strategy. Both the solar PV and battery are installed on DC bus line and hence a converter of suitable size is needed to connect it to the AC load. The simulation constraints ensure that the system has a minimum of two hours of autonomy.

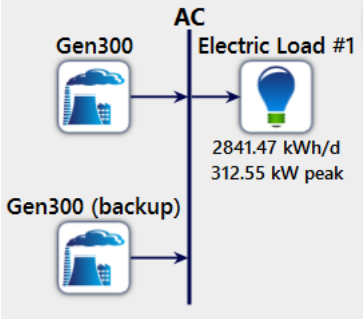

Figure 4.6: Schematic of Scenario 1

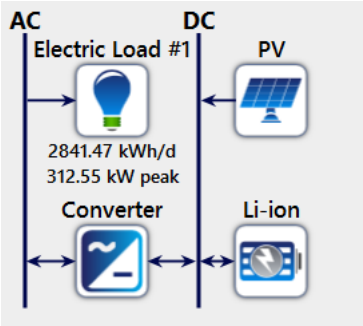

Figure 4.7: Schematic of Scenario 2

The schematic of Scenario 3 is shown in Figure 4.8. It is a 100% renewable power system consisting of solar PV and power to hydrogen (P2H) system including electrolyzer, hydrogen tank and fuel cell. Scenario 3 doesn't have a battery bank. The fuel cell is sized to meet the peak load. The size of the hydrogen storage tank is selected to handle the daily generated hydrogen, plus at least five days of autonomy.

The schematic of Scenario 4 is shown in Figure 4.9. This is a 100% renewable power system as well and includes solar PV generation and a hybrid storage system, which comprises of P2H components and a Li-ion battery bank. The size of the hydrogen tank is selected to handle the daily generated hydrogen, plus at least five days of system autonomy. In this hybrid system, the size of the battery is optimized to handle the peak load for a short period of time, while the P2H system primarily acts like a base-load generator with the component sizes selected so as to utilize the maximum excess energy in the islanded microgrid system.

The scenarios were simulated for optimal component sizes in order to minimize the net

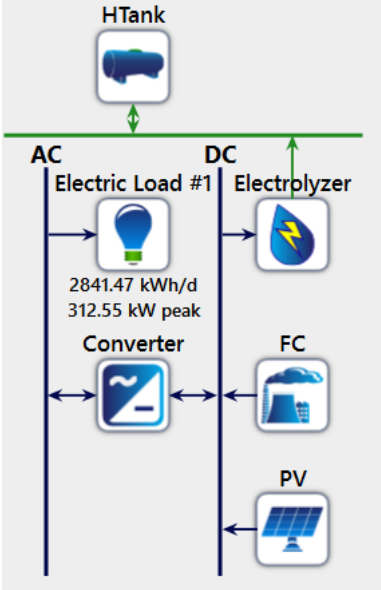

Figure 4.8: Schematic of Scenario 3

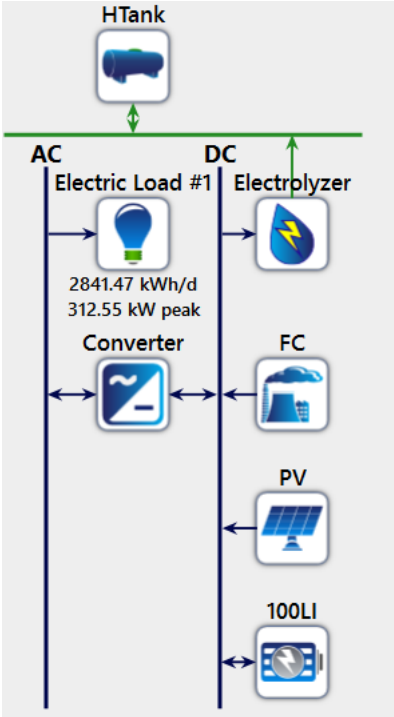

Figure 4.9: Schematic of Scenario 4

present cost of the system. All scenarios were developed to meet the electricity demand with 99.98% reliability and with the least levelized cost of energy in each scenario. Simulation results

are presented in Chapter 5 with a comparative analysis of the different scenarios.

4.4 Input Data

The input parameters for each of the system components which were loaded into HOMER Pro are described in this section. These were used for optimizing the sizing of solar PV, battery storage and converter. For sizing the generators, electrolyzer and the hydrogen storage tank, several discrete sizes were iterated upon to arrive at the most optimal set of system sizes to obtain the least Net Present Cost of the system.

4.4.1 Solar PV panel

A generic flat plate PV system was considered. The input specifications of the PV system are described in Table 4.1.

Table 4.1: Specifications of PV System

Parameter	Value	References
Capital Cost ($/kW) installed	1720	[24]
O&M Cost ($/kW/year)	20	[25]
Replacement Cost ($/kW)	1720	Author estimate
Lifetime (years)	25	[25]
Efficiency (%)	19.1	[25]
Temperature coefficient	-0.39	HOMER Default
Operating temperature	47	HOMER Default

4.4.2 Battery Bank

For the purposes of energy storage, a battery bank is used which maintains the power balance of the system by either storing excess energy or supplying the power deficit. For the present study, the battery bank is composed of Lithium-ion battery package each with

nominal capacity of 100 kWh and round-trip efficiency (RTE) of 90%, respectively. The input specifications of the battery are described in Table 4.2.

Table 4.2: Specifications of Battery Bank

Parameter	Value	References
Type	Lithium-ion	Author defined
Capital Cost ($/kWh) installed	700	[25]
O&M Cost ($/kWh/year)	10	[25]
Replacement Cost ($/kW)	700	Author estimate
Lifetime (years)	15	HOMER Default
Round Trip Efficiency (%)	90	[25]

4.4.3 Bi-directional Converter

The bi-directional converter is used for the regulation of the flow of current into either direction (between AC and DC bus lines). The main function of the converter is to provide power from DC sources to the load. The size of the converter is based on the maximum energy level in the system [26].

4.4.4 Diesel Generator

Two diesel generators with rated capacity of 300 kW each were selected. One of the diesel generators follows the load whereas the other to meet the system load when it exceeds the power of the first generator.

Table 4.3: Specifications of Diesel Generator

Parameter	Value	References
Capital Cost ($) installed	210,000 each	[27]
O&M Cost ($/op. hr)	0.030	[27]
Replacement Cost ($)	210,000	Author estimate
Minimum load ratio	25	HOMER Default
Lifetime (h)	90,000	Author estimate

4.4.5 Fuel Cell

For this study, proton exchange membrane fuel cell (PEMFC) which is widely used in industrial applications and has fast dynamic response [26] has been considered. The input specifications of the fuel cell are described in Table 4.4.

Table 4.4: Specifications of Fuel Cell

Parameter	Value	References
Type	PEMFC	Author defined
Capital Cost ($/kW) installed	2500	[21]
O&M Cost ($/kW/op. hr)	0.020	[28]
Replacement Cost ($/kW)	2500	Author estimate
Efficiency (%) at rated power	62	[28]
Lifetime (h)	60,000	[21]

4.4.6 Electrolyzer

A polymer electrolyte membrane (PEM) type electrolyzer is considered for its merits of technological maturity and acceptable efficiency under different loading conditions. The specifications of the selected electrolyzer are described in Table 4.5.

Table 4.5: Specifications of Electrolyzer

Parameter	Value	References
Type	PEM Electrolyzer	Author defined
Capital Cost ($/kW) installed	2500	[15]
O&M Cost ($/kW/year)	80	[15]
Replacement Cost ($/kW)	2500	Author estimate
Efficiency (%)	85	[29]
Lifetime (years)	15	[15]

4.4.7 Hydrogen Storage Tank

In this study, storage of hydrogen as a compressed gas in durable tanks is considered. The specifications of the selected hydrogen tank are described in Table 4.6.

Table 4.6: Specifications of Hydrogen Tank

Parameter	Value	References
Capital Cost ($/kg H_2) installed	1000	[30],[31]
O&M Cost ($/kg H_2)	10	[30], [31]
Replacement Cost ($/kW)	1000	Author estimate
Lifetime (years)	15	[30], [31]

4.4.8 Project Economics and other optimization inputs

Nominal discount rate for the project lifetime of 25 years is set at 8% and the inflation rate is set to 2%. The simulation time step is specified as one hour to simulate the operation of each system configuration. The system design precision which is the maximum relative precision of decision variables allowed for simulation convergence is set to 0.01 and the net present cost (NPC) precision which is the maximum relative error in NPC required for simulation convergence is also set to 0.01. The value of focus factor which is the setting that controls how evenly HOMER Pro covers the optimization space with points (where each point is a system configuration) is set to a value of 50 on a 0-100 range. A low focus factor covers the space more evenly whereas a high focus factor concentrates points near existing points with a low NPC. Optimizing with a higher focus factor tends to converge more quickly, with fewer total simulations needed, but can risk getting stuck in a local optimum.

Chapter 5

Results and Discussion

5.1 Introduction

This chapter presents the simulation results for each of the four scenarios proposed in Chapter 4. First, the optimization results are presented, which is followed by the sensitivity analysis results. The HOMER Pro optimizer sizes solar PV, battery and generator while the electrolyzer, hydrogen tank and fuel cell capacities are chosen from a list of specified capacities. For each of the four scenarios, HOMER Pro examines different component sizes and selects the components that meet the load requirements as well as the specified system constraints with the least life cycle cost. The four scenarios are then evaluated and compared based on technical, economic and emission related aspects. Sensitivity analysis results with respect to costs of fuel cell and electrolyzer have also been discussed.

5.2 Optimization results for each scenario

Scenario 1: Diesel generator (DG) to meet microgrid load

In this scenario, two options were evaluated (1) a diesel generator with 350 kW capacity and (2) two diesel generators each of capacity 300 kW and the results are summarized in Table 5.1

Table 5.1: Results for Scenario 1. Option 1 considers one 350 kW DG and Option 2 considers two 300 kW DG.

	Results	Option -1	Option-2
Economics	Net Present Cost (million $)	11.0	10.3
	Cost of Energy (25 years) ($/kWh)	0.82	0.76
	Initial Capital Cost (million $)	0.280	0.48
	Operational Cost ($/yr)	830,585	759,853
Electrical	Total electricity production (kWh/yr)	1,156,572	1,097,914
	Excess electricity (kWh/yr)	119,434	60,777
	Total fuel consumed (l)	361,407	335,210
Emissions	Carbon Di-oxide (kg/yr)	953,232	883,014
	Carbon Monoxide (kg/yr)	1,829	1,694
	Sulfur Di-oxide (kg/yr)	2,318	2,148
	Nitrogen Oxides (kg/yr)	9,480	8,781

From the results, it is clear that a load following diesel generator (of 300 kW capacity) plus a secondary generator to meet peak loads (Option-2) is more economical (lower NPC and COE) and environmentally efficient (lower emissions) for the project lifetime of 25 years compared to a single 350 kW capacity generator (Option-1).

As regards the simple pay-back period, the initial capital cost in Option-2 is $200,000 more than Option-1. On the other hand, the operational cost in Option-2 is $70,732/yr less than Option-1. The simple payback time for Option-2 thus evaluates to 2.82 years. Comparing this with the generator lifetime of 90,000 hours (or 10.3 years), Option-2 is economically feasible. Hence, Option-2 is selected for further comparison with other scenarios.

Figure 5.1 shows the efficiency versus output power plot for the two diesel generators

capacities of 300 kW and 350 kW in the lower part of the figure. The upper part of the figure shows the histogram of the microgrid load. It can be seen from the figure that the 300 kW generator is more efficient for the majority of the microgrid load and hence leads to a lower overall cost of energy as is also validated by the Cost of Energy value in Table 5.1.

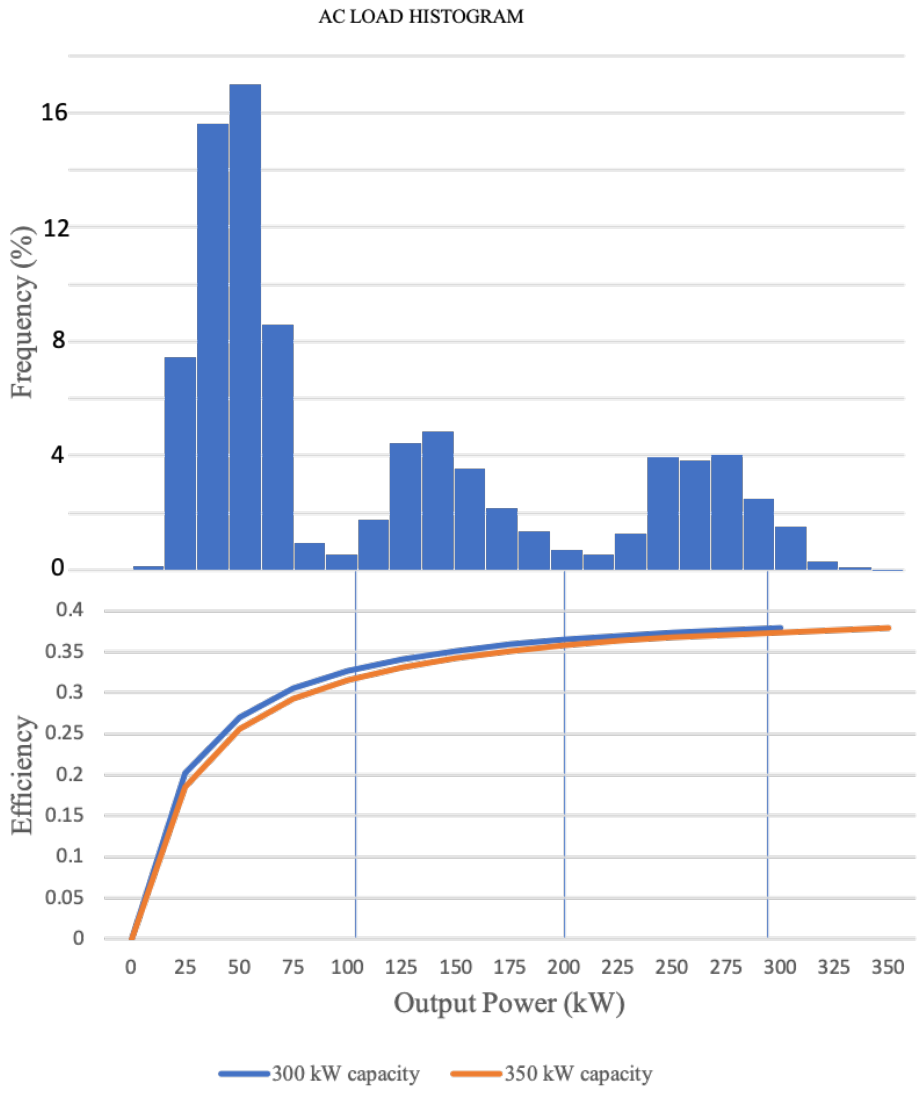

Figure 5.1: Efficiency versus Output Power for 300 kW and 350 kW Diesel Generators. On the top is the histogram of the building load.

Figure 5.2 shows the the distribution of the total system NPC by component and Figure 5.3 shows the the distribution of the total system NPC by cost type for the Option-2. At $2 per

litre of fuel, the diesel fuel cost makes up the majority of the system cost over the project lifetime. The secondary (backup) generator has a lower NPC than the primary generator since it is operated for only around 147 hours/year compared to 8760 hours/year for the primary generator and thus lower O&M and fuel related costs but higher salvage value.

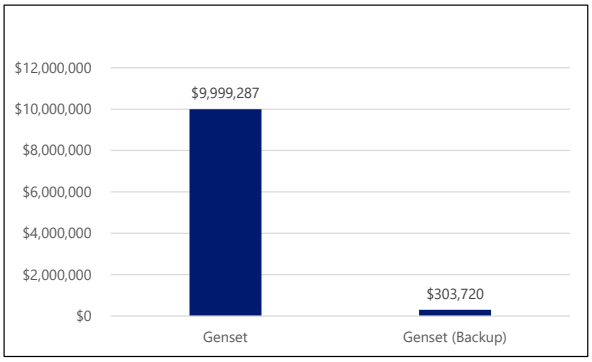

Figure 5.2: Net Present Cost by Component for Scenario 1

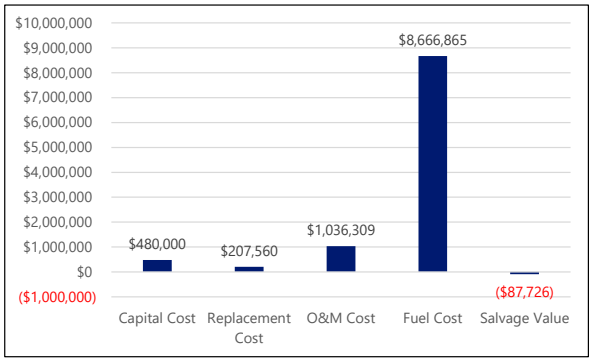

Figure 5.3: Net Present Cost by Cost Type for Scenario 1

Scenario 2: Solar PV + Battery to meet microgrid load

The second scenario uses a renewable energy power source in the form of solar PV and energy storage in the form of Lithium-ion battery bank. The scenario optimization in HOMER Pro led to an optimal system size as shown in Table 5.2 with the least NPC and COE from all different size combinations evaluated by the simulator. The components are chosen such that the system load requirement is met for more than 99.98%.

Figure 5.4 shows the the distribution of the total system NPC by component and Figure 5.5 shows the the distribution of the total system NPC by cost type. The battery cost forms the major proportion (52%) of the system NPC followed by solar PV (46%). Also, it can be seen that this 100% RE system entails high CAPEX but lower OPEX over the project lifetime.

Table 5.2: Results for Scenario 2

Results		
System Component	Solar PV capacity (kW)	2077
	Li-ion Battery Usable Capacity (kWh)	3360
Economics	Net Present Cost (million $)	8.76
	Cost of Energy (25 years) ($/kWh)	0.65
	Initial Capital Cost (million $)	6.63
	Operational Cost ($/yr)	164,989
Electrical	Total electricity production (kWh/yr)	3,347,523
	Excess electricity (kWh/yr)	2,216,685
	Unmet electric load (kWh/yr)	218
	Unmet electric load (%)	0.02
	Capacity shortage (kWh/yr)	252
	Capacity shortage (%)	0.02
Battery	Battery Autonomy (hr)	28.4

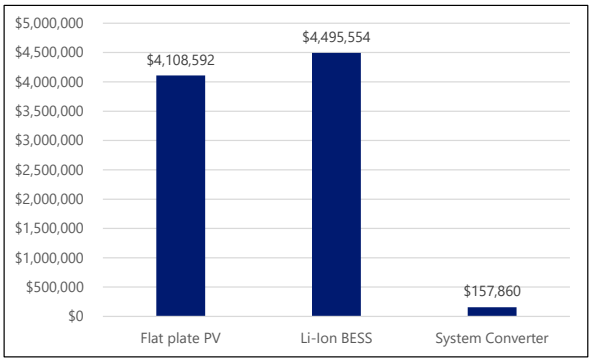

Figure 5.4: Net Present Cost by Component for Scenario 2

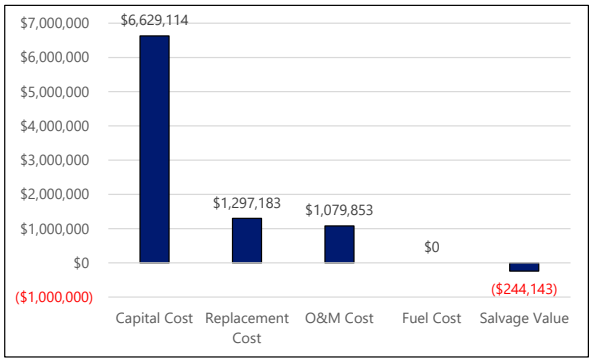

Figure 5.5: Net Present Cost by Cost Type for Scenario 2

Scenario 3: Solar PV + P2H system to meet microgrid load

The third scenario involved using a renewable energy power source in the form of solar PV and a P2H system comprised of electrolyzer, hydrogen storage tank and fuel cell. The system utilized excess renewable electricity to split water into hydrogen (in the electrolyzer) and stored the generated hydrogen in hydrogen storage tank for use by the fuel cell. HOMER Pro optimized the size of solar PV and converter components. For the P2H components, discrete sizes were

specified in the input to enable the simulator to select the most optimal size combination in order to minimize the system NPC and to meet the system reliability of 99.98%. The electrolyzer and the hydrogen tank sizes were selected so as to convert the maximum amount of excess electricity into hydrogen and also to handle the daily generated hydrogen, plus at least five days of autonomy. The fuel cell was sized to meet the daily peak load of 312 kW.

Table 5.3: Results for Scenario 3

Results		
System Component	Solar PV capacity (kW)	2285
	Fuel Cell Capacity (kW)	315
	Electrolyzer Capacity (kW)	750
	H_2 Tank Capacity (kg)	500
Economics	Net Present Cost (million $)	10.80
	Cost of Energy (25 years) ($/kWh)	0.80
	Initial Capital Cost (million $)	7.20
	Operational Cost ($/yr)	281,876
Electrical	Total electricity production (kWh/yr)	4,278,067
	Excess electricity (kWh/yr)	1,857,094
	Unmet electric load (kWh/yr)	309
	Unmet electric load (%)	0.02
	Capacity shortage (kWh/yr)	300
	Capacity shortage (%)	0.02
H_2 storage tank	H_2 Tank Autonomy (hr)	141

Figure 5.6 shows the distribution of the total system NPC by component and Figure 5.7 shows the the distribution of the total system NPC by cost type. Solar PV system makes up 42% of the system NPC while P2H components form the major proportion of the system NPC (58%) and amongst them PEM electrolyzer cost dominating at 31%. This 100% RE system entails high CAPEX but lower OPEX over the project lifetime.

Scenario 4: Solar PV + Battery + P2H system to meet microgrid load

The final scenario uses a renewable energy power source in the form of solar PV and a hybrid energy storage system comprising of Lithium-ion battery and hydrogen storage along with

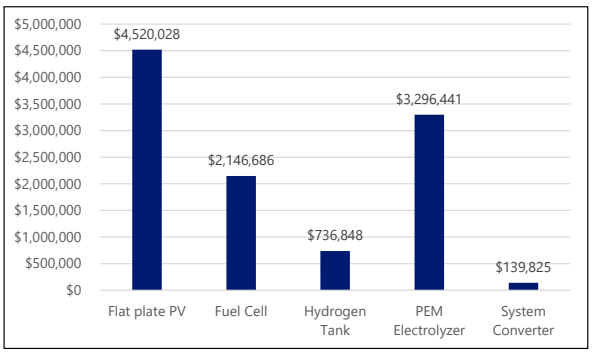

Figure 5.6: Net Present Cost by Component for Scenario 3

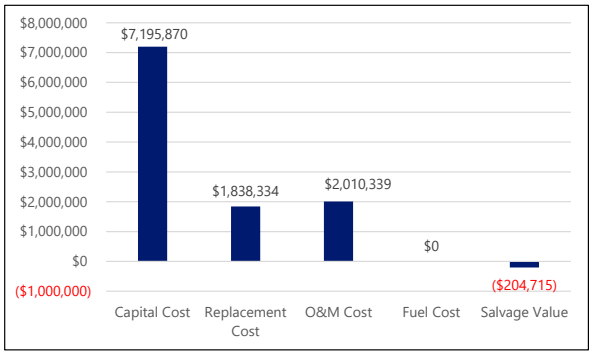

Figure 5.7: Net Present Cost by Cost Type for Scenario 3

the other P2H system components including the electrolyzer and fuel cell to enhance the system flexibility as well as system autonomy. The size of the hydrogen tank is selected to handle daily generated hydrogen, plus at least five days of system autonomy. The evaluation results of this scenario are shown in Table 5.4. The components are chosen such that the system reliability is 99.98%.

Figure 5.8 shows the the distribution of the total system NPC by component and Figure 5.9 shows the the distribution of the total system NPC by cost type. Solar PV makes up 10% of the system NPC. It can be seen that the P2H components form the major proportion of the system NPC (76%) and amongst them hydrogen tank cost dominating at 42%, followed by fuel cell cost at 22%, and PEM electrolyzer cost at 12%. This 100% RE system entails high CAPEX but lower OPEX over the project lifetime.

5.3 Comparison of results

Table 5.5 shows the simulation results for each of the four scenarios based on the given inputs and constraints discussed in Chapter 4.

The Net Present Cost (NPC) is least for Scenario 4 whereas it is the highest for Scenario 1

Table 5.4: Results for Scenario 4

Results		
System Component	Solar PV capacity (kW)	1661
	Li-ion Battery Nominal Capacity (kW)	560
	Fuel Cell Capacity (kW)	250
	Electrolyzer Capacity (kW)	400
	H_2 Tank Capacity (kg)	600
Economics	Net Present Cost (million $)	7.80
	Cost of Energy (25 years) ($/kWh)	0.58
	Initial Capital Cost (million $)	5.68
	Operational Cost ($/yr)	164,008
Electrical	Total electricity production (kWh/yr)	2,963,161
	Excess electricity (kWh/yr)	1,213,498
	Capacity shortage (kWh/yr)	338
	Capacity shortage (%)	0.02
	Capacity shortage (kWh/yr)	330
	Capacity shortage (%)	0.02
Autonomy	H_2 storage tank autonomy (h)	169
	Battery autonomy (h)	4.73

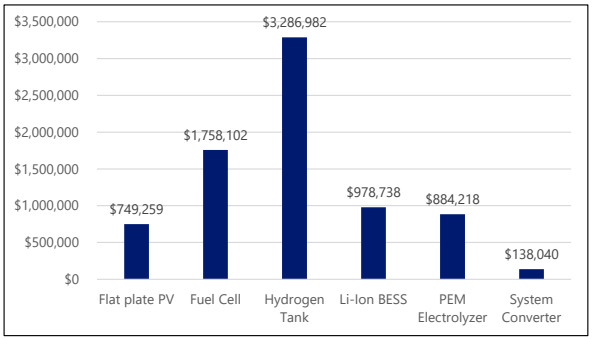

Figure 5.8: Net Present Cost by Component for Scenario 4

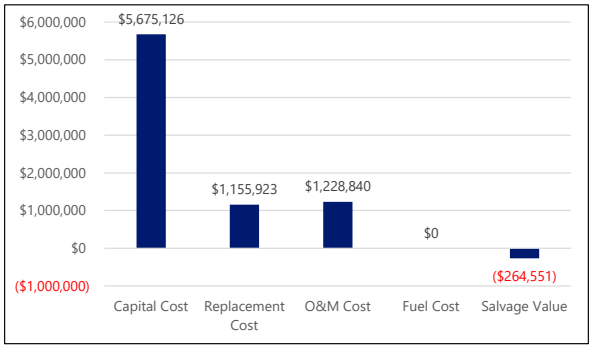

Figure 5.9: Net Present Cost by Cost Type for Scenario 4

(base-case). Scenario 1 also has the highest levelized cost of energy (COE) evaluated over the project lifetime of 25 years. Moreover, it is also the highest in emissions (883 metric tons CO_2 per year) due to diesel fuel consumption and absence of any renewable energy component in the energy mix.

Table 5.5: Simulation results for the proposed scenarios

	Results	Scenario 1	Scenario 2	Scenario 3	Scenario 4
System Component	Solar PV capacity (kW)	X	2077	2285	1661
	DG 1 capacity (kW)	300	X	X	X
	DG 2 capacity (kW)	300	X	X	X
	Li-ion battery capacity (kWh)	X	3360	X	560
	Fuel cell capacity (kW)	X	X	315	250
	Electrolyzer capacity (kW)	X	X	750	400
	H_2 tank capacity (kg)	X	X	500	600
	Converter capacity (kW)	X	391	347	342
Economics	Total Net Present Cost (million $)	10.3	8.76	10.80	7.80
	Cost of Energy (25 years) ($/kWh)	0.76	0.65	0.80	0.58
	Initial Capital Cost (million $)	0.48	6.63	7.20	5.68
	Operational Cost ($/yr)	759,853	164,989	281,876	164,008
Electrical	Renewable Energy fraction (%)	0	100	100	100
	Capacity shortage (kWh/yr)	0	252	300	330
	Capacity shortage (%)	0	0.02	0.02	0.02
	Excess electricity (kWh/yr)	60,777	3,065,109	2,091,706	1,213,498
	Excess electricity (%)	5.54	66.2	43.4	41.0
	Dispatch strategy	LF	LF	LF	LF
	Total electricity production (kWh/yr)	1,097,914	3,347,523	4,278,067	2,963,161
Diesel Generator	DG 1 operating (hours/yr)	8760	X	X	X
	DG 2 operating (hours/yr)	147	X	X	X
Fuel Cell and Electrolyzer	Fuel cell operating (hours/yr)	X	X	7114	3366
	Fuel cell capital cost (million $)	X	X	2.14	1.76
	Fuel cell H_2 fuel (kg)	X	X	28,236	13,450
	Electrolyzer Capital Cost (million $)	X	X	3.29	0.88
H_2 storage tank	H_2 tank autonomy (hr)	X	X	141	169
Battery	Battery autonomy (hr)	X	28.4	X	4.73
	Battery usable capacity (kWh)	X	3360	X	560

Comparing Scenarios 1 and 2, we see that the renewable energy system in Scenario 2 has a higher CAPEX but lower OPEX value than Scenario 1 which shows that the elimination of emissions from diesel generators by using solar PV and battery storage components requires higher initial capital costs but lower operational costs. However, COE in Scenario 2 is lower than in Scenario 1 by 16% over the considered project duration of 25 years. In order to optimize sizes of solar PV array and battery storage towards obtaining the least NPC and COE as well as ensuring system reliability which means ensuring that the batteries are sufficiently charged to

cover the demand during periods of poor solar resource / night time, a large solar PV generation capacity was required (2077 kW) . This led to an excess generated electricity of 66% in Scenario 2. The system autonomy in Scenario 2 is about 28 hours due to installation of battery storage and a higher capacity battery (thereby entailing higher investment) would be required to reduce curtailment. Scenarios 3 and 4 include a power to hydrogen (P2H) system. The simulation results reveal that Scenario 3 is worse in terms of overall COE and NPC when compared to Scenario 4 which indicates that large P2H system is more costly than a P2H-Battery hybrid system. The presence of a hydrogen tank, however, for storing excess renewable energy is more effective than a battery system in terms of the system autonomy- it is 169 hours for Scenario 3 as against 28 hours for Scenario 2 and 141 hours for Scenario 4. With regards to solar PV capacity, we see that relatively smaller sized solar PV array is required for the same energy balance. Both Scenarios 3 and 4 also have significantly lower COE and NPC compared to Scenario 1. Scenario 4 comprises of a much smaller battery capacity compared to Scenario 2. The battery here functions to mainly handle peak loads for a short period of time. The fuel cell is sized to 315 kW in Scenario 3 to meet the system peak of 312 kW.

Figure 5.10 illustrates the system operation of the P2H-Battery hybrid system in Scenario 4 for one week in a high solar radiation summer month of June. The plot demonstrates the contribution of hydrogen fuel to power the system using the fuel cell for long hours. The hydrogen capacity in the storage tank is at a high level since excess electricity generation is used to produce hydrogen by the electrolyzer. The electric battery is rarely used.

Figure 5.11 illustrates the system operation of the P2H-Battery hybrid system in Scenario 4 for one week in a low solar radiation winter month of December. The hydrogen capacity in the tank fluctuates due to occasional poor solar radiation.

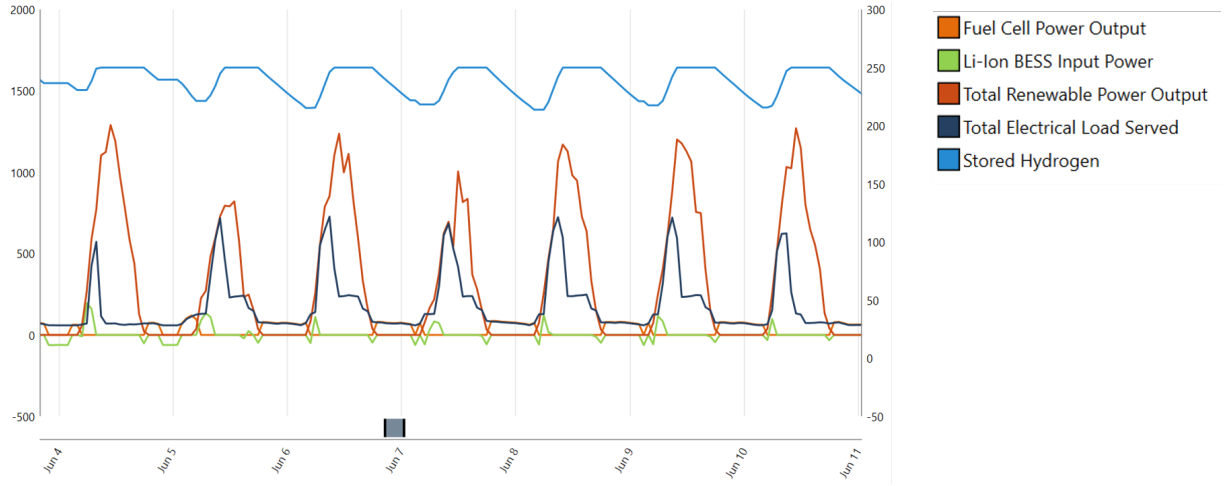

Figure 5.10: One week Load Profile (June)

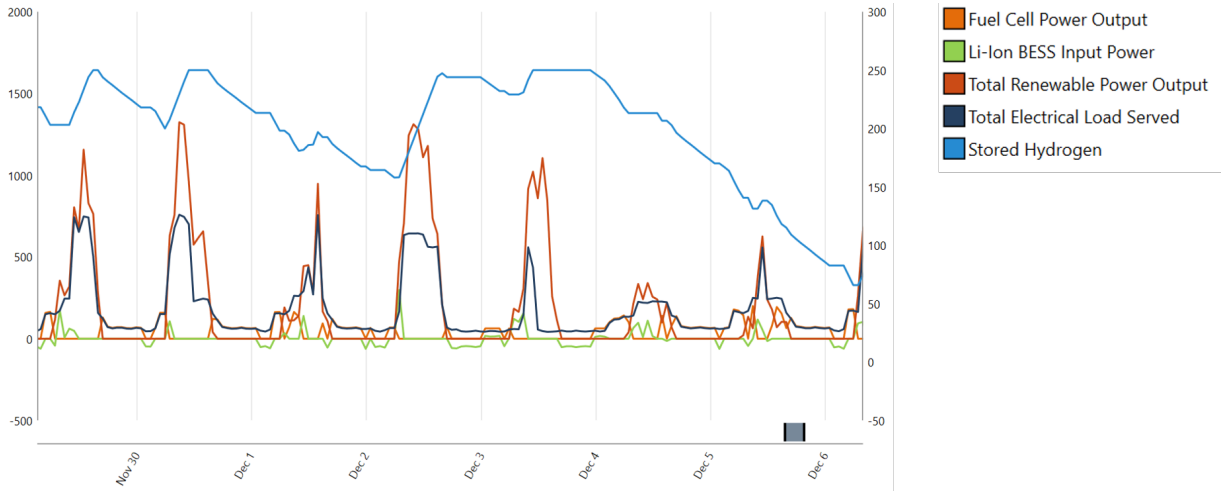

Figure 5.11: One week Load Profile (December)

5.4 Sensitivity analysis

The majority of the project cost - total project capital cost and cost of energy in Scenario 4 was incurred by the P2H components, in particular the Electrolyzer and the Fuel Cell and hence a sensitivity analysis for the impact of each component's capital cost on the total project's net present cost and levelized cost of energy (LCOE) was conducted.

From Figure 5.12, it can be seen how the cost of energy as well as the total net present cost reduces with reduction in the electrolyzer and fuel cell capital cost.

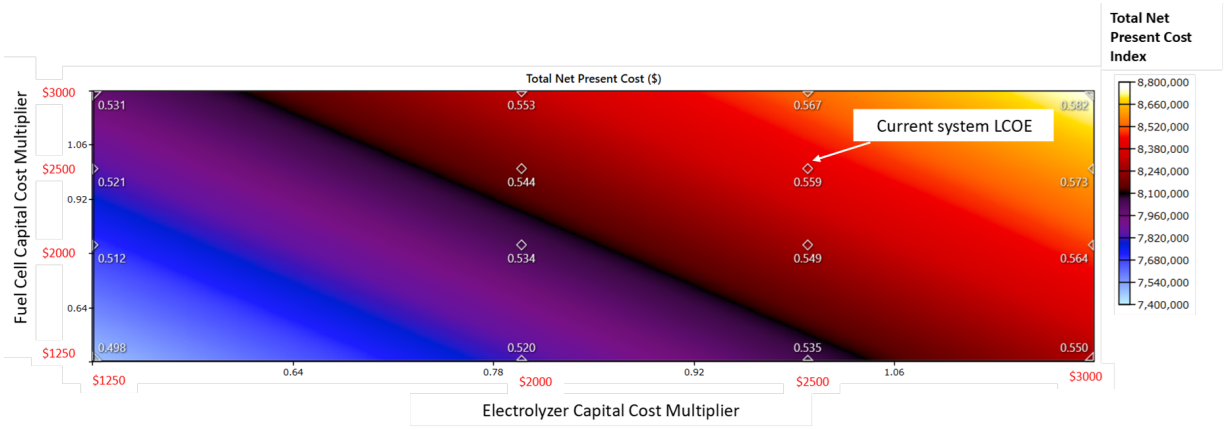

Figure 5.12: Cost sensitivity of electrolyzer and fuel cell. X-axis denotes the electrolyzer capital cost multiplier (numbers in red are capital cost values in ($)). Y axis denotes the fuel cell capital cost multiplier (numbers in red are capital cost values in ($)). Numbers in white overlapping the colored plot indicate total system cost of energy, LCOE. The color index indicates the magnitude of total net present cost.

We can see that, reduction in capital cost of electrolyzer and fuel cell by $500/kW (20%) each will reduce LCOE by 4% and system net present cost by 7% and reduction in capital cost of electrolyzer and fuel cell by $1250/kW (50%) each will reduce LCOE by 10% and system net present cost by 14%.

5.5 Discussion of results

HOMER Pro optimally sized the solar PV, battery and converter components based on the system inputs and constraints. For electrolyzer, hydrogen tank and fuel cell, it selected the most optimal component size from the list of sizes specified during the input stage so as to achieve the least system life cycle cost.

The hydrogen-battery hybrid system in Scenario 4 uses a smaller sized battery system compared to Scenario 2. This battery besides being used to handle peak loads for short duration, could also be used for ancillary operations like system frequency and voltage control in the microgrid.

As seen from Scenarios 3 and 4, while hydrogen storage is a promising approach to enhance the system autonomy, there are still some techno-economic challenges like high inflammability necessitating expenditure on safety related infrastructure, full load inappropriateness, and high capital investment in the system that need to be addressed before the technology can be fully commercialised for grid scale storage applications. The sensitivity analysis results indicate that cost reduction in P2H components increases the economic feasibility of integrating these components into the existing renewable systems with the added benefits of long term storage and enhanced system autonomy (on account of hydrogen storage) which is essential for a stand-alone microgrid operation.

Chapter 6

Conclusions

In this study, a set of 100% renewable energy scenarios (battery based, hydrogen based and hybrid combination of battery and hydrogen based) were defined, modeled and simulated for a stand-alone microgrid and compared with a base-case scenario of diesel generators meeting the microgrid load. Based on simulation using HOMER Pro, the following main conclusions could be drawn:

- The evaluation of all scenarios demonstrated that the P2H-battery hybrid combination based scenario (Scenario 4) is the most promising approach for the selected 100% renewable energy based stand alone microgrid site in San Diego, California
- The hybrid system leads to less curtailment of excess electricity compared to battery-only storage system
- The hybrid system is able to extend the system autonomy compared to a battery-only storage system in the form of stored hydrogen

The production of hydrogen from renewable energy sources could be the solution to long-term energy storage and provide an energy vector with a variety of uses and excellent environmental characteristics. In particular, hydrogen could be further converted into synthetic

methane by using carbon dioxide from Anaerobic Digester plants which could be injected into Natural Gas pipelines, could be used in heating applications, and in fuel cell vehicle applications with almost zero emissions. Future work aims at analysing the technical and cost benefits of including these further hydrogen-use pathways.

Bibliography

[1] G.J. Dalton, D.A. Lockington, and T.E. Baldock. Feasibility analysis of stand-alone renewable energy supply options for a large hotel. *Renewable Energy*, 33(7):1475–1490, 2008.

[2] Alireza Haghighat Mamaghani, Sebastian Alberto Avella Escandon, Behzad Najafi, Ali Shirazi, and Fabio Rinaldi. Techno-economic feasibility of photovoltaic, wind, diesel and hybrid electrification systems for off-grid rural electrification in colombia. *Renewable Energy*, 97:293–305, 2016.

[3] Alessandro Corsini, Franco Rispoli, Mario Gamberale, and Eileen Tortora. Assessment of h2- and h2o-based renewable energy-buffering systems in minor islands. *Renewable Energy*, 34(1):279–288, 2009.

[4] Mariya Soshinskaya, Wina H.J. Crijns-Graus, Jos van der Meer, and Josep M. Guerrero. Application of a microgrid with renewables for a water treatment plant. *Applied Energy*, 134:20–34, 2014.

[5] Li He, Shiyue Zhang, Yizhong Chen, Lixia Ren, and Jing Li. Techno-economic potential of a renewable energy-based microgrid system for a sustainable large-scale residential community in beijing, china. *Renewable and Sustainable Energy Reviews*, 93:631–641, 2018.

[6] Samir M. Dawoud, Xiangning Lin, and Merfat I. Okba. Hybrid renewable microgrid optimization techniques: A review. *Renewable and Sustainable Energy Reviews*, 82(3):2039–2052, 2018.

[7] Jingfeng Chen, Ping Yang, Jiajun Peng, Yuqi Huang, Yaosheng Chen, and Zhiji Zeng. An improved multi-timescale coordinated control strategy for stand-alone microgrid with hybrid energy storage system. *Energies*, 11(8):2150, 2018.

[8] Jianwei Li, Rui Xiong, Qingqing Yang, Fei Liang, Min Zhang, and Weijia Yuan. Design/test of a hybrid energy storage system for primary frequency control using a dynamic droop method in an isolated microgrid power system. *Applied Energy*, 201:257–269, 2017.

[9] G.M. Shafiullah, M.T.O. Amanullah, A.B.M. Shawkat Ali, Dennis Jarvis, and Peter Wolfs. Prospects of renewable energy – a feasibility study in the australian context. *Renewable Energy*, 39(1):183–197, 2012.

[10] E.I. Zoulias and N. Lymberopoulos. Techno-economic analysis of the integration of hydrogen energy technologies in renewable energy-based stand-alone power systems. *Renewable Energy*, 32(4):680–696, 2007.

[11] Furat Dawood, GM Shafiullah, and Martin Anda. Stand-alone microgrid with 100% renewable energy: A case study with hybrid solar pv-battery-hydrogen. *Sustainability*, 12(5), 2020.

[12] Paolo Colbertaldo, Stacey Britni Agustin, Stefano Campanari, and Jack Brouwe. Impact of hydrogen energy storage on california electric power system: Towards 100% renewable electricity. *International Journal of Hydrogen Energy*, 44(19):9558–9576, 2019.

[13] Sebastian Schiebahn, Thomas Grube, Martin Robinius, Vanessa Tietze, Bhunesh Kumar, and Detlef Stolten. Power to gas: Technological overview, systems analysis and economic assessment for a case study in germany. *International Journal of Hydrogen Energy*, 40(12):4285–4294, 2015.

[14] M. M. Rashid, M. K. Al Mesfer, and M. Naseem, H. & Danish. Hydrogen production by water electrolysis: a review of alkaline water electrolysis, pem water electrolysis and high temperature water electrolysis. *International Journal of Engineering and Advanced Technology*, 2015.

[15] Ahmad Mayyas, Mark Ruth, Bryan Pivovar, Guido Bender, and Keith Wipke. Manufacturing cost analysis for proton exchange membrane water electrolyzers. *NREL/TP-6A50-72509*, https://www.nrel.gov/docs/fy19osti/72509.pdf, 2019.

[16] Sun X, Simonsen SC, Norby T, and Chatzitakis A. Composite membranes for high temperature pem fuel cells and electrolysers: A critical review. *Membranes (Basel)*, 2019.

[17] Frano Barbir. Pem electrolysis for production of hydrogen from renewable energy sources. *Solar Energy*, 78(5):661–669, 2005.

[18] Hanane Dagdougui, Roberto Sacile, Chiara Bersani, and Ahmed Ouammi. *Chapter 4 - Hydrogen Storage and Distribution: Implementation Scenarios, Hydrogen Infrastructure for Energy Applications*. Academic Press, 2018.

[19] https://www.hydrogenics.com/technology-resources/hydrogen-technology/fuel-cells/. Accessed on June 1, 2020.

[20] H. Ren and J. Chae. Fuel cells technologies for wireless mems. *Wireless MEMS Networks and Applications*, 2017.

[21] Vince Contini, Fritz Eubanks, Mike Heinrichs, Manoj Valluri, Mike Jansen, Paul George, and Mahan Mansouri. Manufacturing cost analyses of fuel cell systems for primary power and combined heat and power applications. *Battelle*, https://www.energy.gov/sites/prod/files/2017/05/f34/fcto_bop_workshop_contini.pdf, 2017.

[22] Felix A. Farret and M. Godoy Simões. Micropower system modeling with homer. *Integration of Alternative Sources of Energy*, pages 379–418, 2006.

[23] J. A. Duffie and W. A. Beckman. *Solar Engineering of Thermal Processes 2nd ed.* Wiley, 1991.

[24] Ran Fu, David Feldman, and Robert Margolis. Us solar photovoltaic system cost benchmark q1 2018. *NREL/TP-6A20-68925*, https://www.nrel.gov/docs/fy19osti/72399.pdf, 2018.

[25] Dylan Cutler, Dan Olis, Emma Elgqvist, Xiangkun Li, Nick Laws, Nick DiOrio, Andy Walker, and Kate Anderson. Reopt: A platform for energy system integration and optimization. *NREL/TP-7A40-70022*, 2017.

[26] Vendoti Suresh, Muralidhar M., and R. Kiranmayi. Modelling and optimization of an off-grid hybrid renewable energy system for electrification in a rural areas. *Energy Reports*, 6(1):594–604, 2020.

[27] Sean Ericson and Dan Olis. A comparison of fuel choice for backup generators. *NREL/TP-6A50-72509*, 2019.

[28] Brian D. James, Daniel A. DeSantis, and Genevieve Saur. Final report: Hydrogen production pathways cost analysis (2013 – 2016). *DOE-StrategicAnalysis-6231-1*, https://www.osti.gov/servlets/purl/1346418, 2016.

[29] S. Shiva Kumar and V. Himabindu. Hydrogen production by pem water electrolysis – a review. *Materials Science for Energy Technologies*, 2(3):442–454, 2019.

[30] Dr. Timothy E. Lipman, Mr. Ryan Ramos, , and Professor Daniel M. Kammen. An assessment of battery and hydrogen energy storage systems integrated with wind energy resources in california. *California Energy Commission, Public Interest Energy Research (PIER) Program*, 6(1):594–604, 2005.

[31] Rodica Loisel, Laurent Baranger, Nezha Chemouri, Stefania Spinu, and Sophie Pardo. Economic evaluation of hybrid off-shore wind power and hydrogen storage system. *International Journal of Hydrogen Energy*, 40(21):6727–6739, 2015.